Tetrahedron 67 (2011) 7148–7155

Contents lists available at ScienceDirect

Tetrahedron

journal homepage: www.elsevier.com/locate/tet

Synthesis of thiophene-substituted aza-BODIPYs and their optical and electrochemical properties

Roland Gresser, Horst Hartmann *, Marion Wrackmeyer, Karl Leo, Moritz Riede

Institut für Angewandte Photophysik, George-Bähr-Str. 1, Technische Universität Dresden, 01062 Dresden, Germany

ARTICLE INFO

Article history:
Received 23 March 2011
Received in revised form 20 June 2011
Accepted 27 June 2011
Available online 2 July 2011

Keywords:
Aza-BODIPY
Stille-coupling
NIR absorption
Cyclic voltammetry
DFT calculations

ABSTRACT

A series of novel thiophene-substituted aza-BODIPY dyes were synthesized by means of a standard procedure and complemented by a Stille-coupling of a brominated species with 2-tributylstannylthiophene. The optical as well as the electrochemical properties of the compounds were investigated and compared to result of density functional theory (DFT) calculations. The influence of the thiophene substituents is discussed in dependence of the position at the aza-BODIPY core regarding the HOMO and LUMO frontier orbitals. The different distributions of the HOMO and LUMO coefficients over the BODIPY core lead to a variable influence of the thiophene substituents on the HOMO and LUMO energies, being the origin of the tunable optical and electrochemical properties.

1. Introduction

Boron difluoride dipyrromethene derivatives (BODIPYs) have attracted much attention due to their intense absorption and strong fluorescence combined with an excellent photostability.[1] Therefore, a large range of divers substituted BODIPYs have been prepared and extensively studied for various applications, such as fluorescence probes, e.g., for biological imaging,[2] as emitter material in organic light emitting diodes,[3] or as absorber material for organic solar cells.[4]

In contrast, corresponding aza-BODIPYs as aza-analogous BODIPYs (Scheme 1) are described to a lower extent in the literature hitherto, obviously due to their less effective synthesis starting from 1,3-bis(het)aryl-4-nitrobutanones[5] or from 1-(het)aryl-5-nitroso-pyrroles.[6] Nevertheless, few aza-BODIPYs have been studied for some applications, such as sensitizers for singlet oxygen generation,[7] as near-infrared absorbers,[8] as NIR-emitting chemosensors for heavy-metal detection,[9] or as fluorescent sensors for polymer characterization.[10]

Because thienyl-substituents at the BODIPY core give rise to compounds with some interesting properties, e.g., to compounds with remarkable long-wavelength absorptions[11] and emissions,[12] to redox-active polymers,[13] to heavy-metal sensors,[14] or to light-collectors,[15] on the one hand, and thienyl-substituted aza-BODIPY derivatives are unknown at yet, on the other hand, we have synthesized few examples **1a**–**d** of this series and studied their optical and electrochemical properties more in detail. In addition to the experimental studies, quantum chemical calculations by means of the density functional theory (DFT) were applied to obtain deeper insights into their absorption characteristics and energy levels, which are essential for understanding the optoelectronic properties of these compounds.

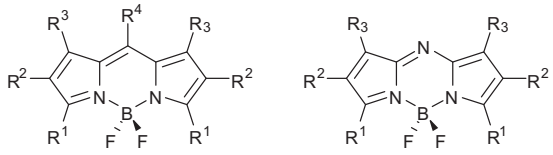

Scheme 1. Representation of the BODIPY (difluoroboradiaza-indacene) and the aza-BODIPY (difluoroboratriaza-indacene) structures.

2. Results and discussion

2.1. Synthesis

The synthesis of the thiophene-substituted aza-BODIPYs **1a**–**d** (see Scheme 2) follows a route developed by Rogers[5] in 1943 and later on applied for other aza-BODIPYs as well.[5,6,7a,8c,9]

In the crucial step of this method (outlined in Scheme 3), 4-nitro-1,3-di(het)arylbutanones **6** are reacted with ammonium

* Corrresponding author. E-mail address: hartmann@iapp.de (H. Hartmann).

0040-4020/$ – see front matter © 2011 Elsevier Ltd. All rights reserved.
doi:10.1016/j.tet.2011.06.100

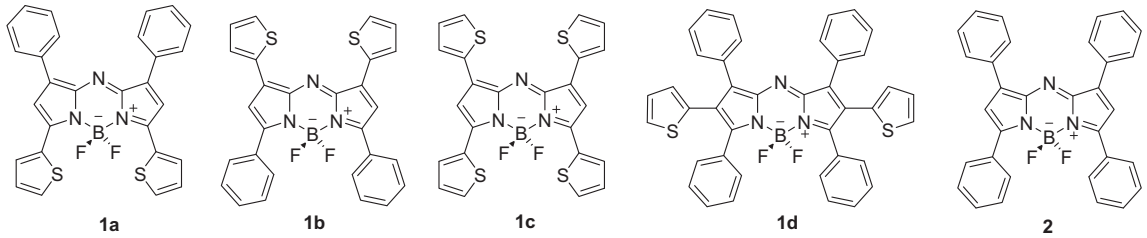

Scheme 2. Thiophene-substituted aza-BODIPYs **1a**–**d** investigated in comparison to the tetraphenyl-substituted parent compound **2**.

acetate to the appropriate pyrroles and nitroso-pyrroles, as demonstrated by Hall et al.,[6] followed by a subsequent condensation of both intermediates.

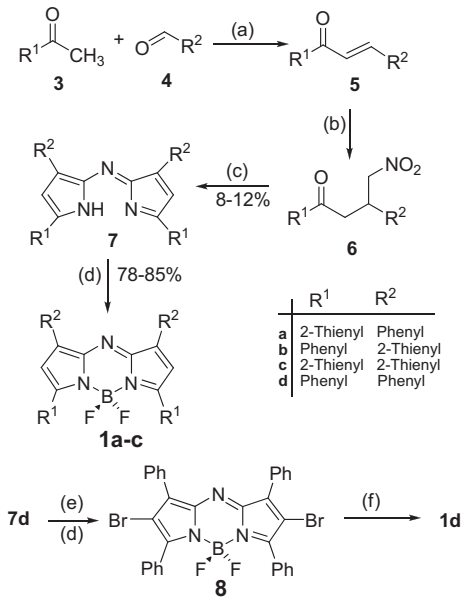

Scheme 3. Synthetic routes to the thienyl-substituted aza-BODIPYs **1a**–**d**. (a) KOH in EtOH, rt, (b) CH_3NO_2 in EtOH, K_2CO_3, reflux, (c) BuOH, NH_4HOAc, reflux, (d) $BF_3 \cdot Et_2O$, dichloroethane, DIPEA, reflux, (e) Br_2, benzene, rt, (f) 2-tributylstannyl-thiophene, $Pd(PPh_3)_4$, toluene, reflux.

The necessary 4-nitro-1,3-di(het)arylbutanones **6** are readily available by a base-mediated Michael-addition of nitro methane to a thiophene substituted chalcone **5**. After aqueous work-up, the reaction gave nearly quantitative yields of 4-nitro-1,3-di(het)arylbutanones **6**, which were directly used without further purification. The required substituted chalcones **5** were synthesized in the first step via an aldol condensation of (het)arylketones **3** with (het) arylaldehydes **4** in excellent yields.[16]

By using this procedure, the dipyrroazamethenes **7a**–**c** were obtained in yields of 6–12%. Finally, the desired thiophene-substituted aza-BODIPYs **1a**–**c** were prepared by reaction of the azamethenes **7a**–**c** with boron trifluoride etherate under standard conditions in good yields ranging between 71% and 82%.

For the synthesis of the star-shaped 2,5-dithienyl substituted aza-BODIPY **1d** an extended route using the dibromo aza-BODIPY compound **8** as key intermediate has been used. This dibromo compound **8** was prepared according to a route described by O'Shea et al.[7,17] and transformed in good yields into the target compound **1d** by means of a Stille-coupling using 2-tributylstannyl-thiophene as co-reactant.

2.2. Spectroscopic characteristics

The spectroscopic data of all aza-BODIPYs **1a**–**d** and their boron free precursors **7a**–**d** are summarized in Table 1. The corresponding spectra are depicted in Fig. 1. The 1,3,5,7-tetraphenyl aza-BODIPY **2**, which was already described elsewhere,[14,17] is shown here for reasons of comparison.

Table 1
Spectroscopic characteristics of the dipyrromethines **7a**–**d** and aza-BODIPY compounds **1a**–**d**, measured in dichloromethane

	λ uv[a] [nm]	Extinction [L mol^{-1} cm^{-1}]	λ_{max}[b] [nm]	Extinction [L mol^{-1} cm^{-1}]	λ_{flu} [nm][c]	Φ[d]
7a	328	35,500	633	43,000	—	—
7b	308	36,000	625	37,500	—	—
7c	335	37,500	663	45,000	—	—
7d	297	42,500	590	40,000	—	—
1a	344	35,000	718	120,500	740 (22)	0.44
1b	320	29,000	683	78,000	725 (42)	0.10
1c	354	40,000	742	110,000	764 (22)	0.11
1d	270	18,500	650	40,000	—	—

[a] Extinction coefficients are given for the most intense absorption in the UV region of the spectra.
[b] The absorption maximum in the visible regime.
[c] Stokes-shifts are specified in brackets.
[d] Fluorescence quantum yield measured relative to the one of Rhodamine 101.

The absorption spectra of all dipyrroazamethenes **7a**–**d** exhibit two intense peaks, one in the UV region (which is the maximum in case of **7d**) and one in the visible region (usually the maximum).

The absorption maxima of the thiophene substituted dipyrroazamethenes **7a**–**c** are found in the visible region at 633 nm, 625 nm, and 663 nm, respectively. These maxima are significantly shifted into the red region compared to the 1,3,5,7-tetraphenyl substituted dipyrroazamethene **7d**, which absorbs at 589 nm.[14,17] The extinctions of both absorption peaks in the UV and the visible are similar for all dipyrroazamethenes **7a**–**d** and found to be between 35,000 and 37,000 L mol^{-1} cm^{-1} for the first absorption bands and between 40,000 and 45,000 L mol^{-1} cm^{-1} for the second bands, as can be seen in Table 1.

The complex formation of the dipyrroazamethenes **7** with boron trifluoride has a tremendous influence on the absorption characteristics of the resulting thiophene-substituted aza-BODIPYs **1a**–**d**. It gives rise to a strong bathochromic shift, especially for the compounds **1a**–**c** bearing the thiophene substituents in the 1,7- or/and 3,5-positions (see Table 1). Such a bathochromic shift is known in the BODIPY series to be caused by the complexation with boron trifluoride[17,18] but it is unusual strong for **1a** and **1c** with 85 nm and 79 nm, since for the 1,3,5,7-tetraphenyl aza-BODIPY **2** it amounts only to 61 nm compared to the corresponding borondi fluoride-free 1,3,5,7-tetraphenyl dipyrroazamethene.[17]

As a result, by replacing the phenyl moieties in 1,3,5,7-positions at the aza-BODIPY core by thiophene moieties (compare **1c** and **2**), the absorption maximum can be shifted bathochromically by 92 nm. Surprisingly, compound **1d** with the thiophene substituent in the 2,6-positions at the aza-BODIPY core shows the most hypsochromic and most broadened absorbance in this series with an absorption maximum at 650 nm. This value is the same as for compound **2**[17] and indicates that the thiophene moieties at the 2,6-positions do not have any influence on the visible spectral part. However, in the UV part of the spectrum of **1d**, the absorption band

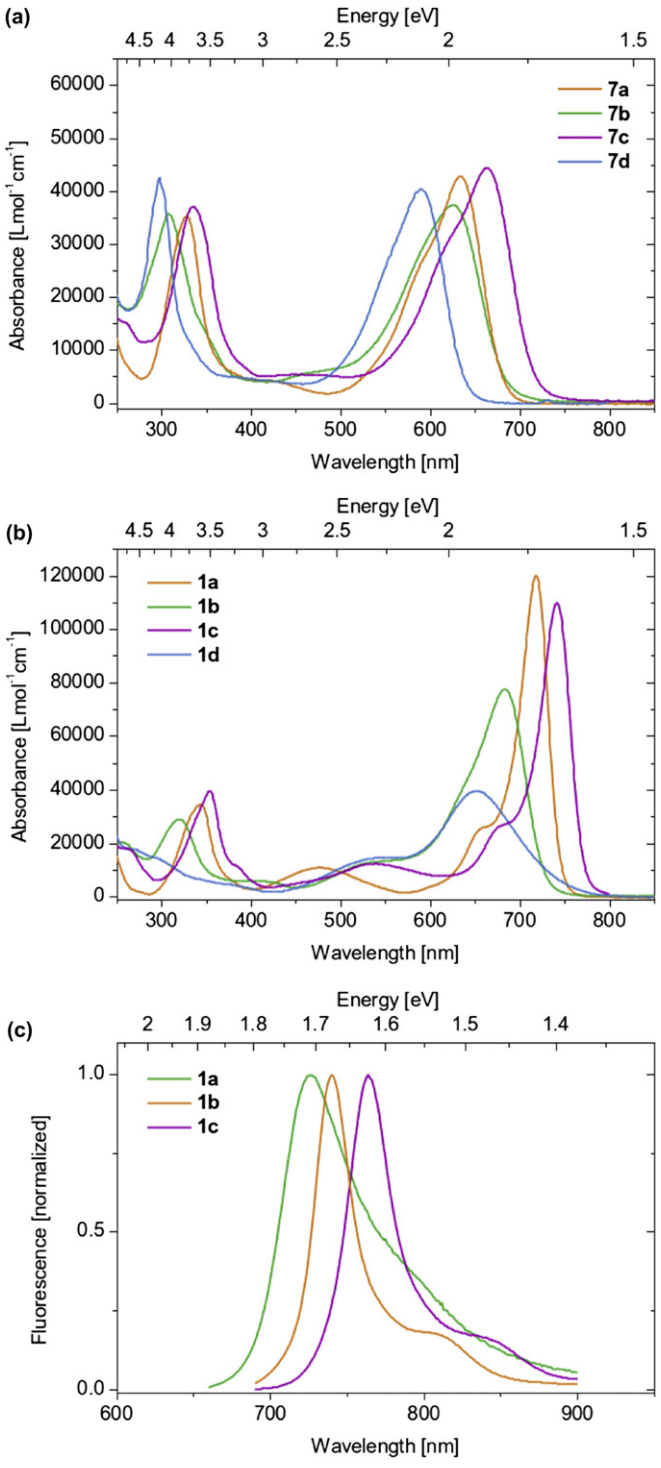

Fig. 1. Spectroscopic characteristics for **7a**–**d** and **1a**–**d**; (a) absorption spectra of the boron free compounds **7a**–**d**; (b) absorption spectra of the boron difluoride complexes **1a**–**d**; (c) fluorescence spectra of **1a**–**c**. Compound **1d** did not show any measurable fluorescence. For details on the wavelength and the extinction coefficients see Table 1.

is diminished, what is in contrast to the other thiophene-substituted aza-BODIPYs **1a**–**c**.

The extinctions of the thiophene-substituted aza-BODIPYs **1a**–**d** differ significantly in dependence of the substitution pattern. The strongest extinction with 120,000 L mol^{-1} cm^{-1} is found for the 3,5-dithienyl-substituted aza-BODIPY compound **1a**, followed by the 1,3,5,7-tetrathienyl derivative **1c** with 110,000 L mol^{-1} cm^{-1}. The 1,7-dithienyl-substituted species **1b** shows a weaker absorbance with 78,000 L mol^{-1} cm^{-1}. The 2,6-dithienyl substitution in the aza-BODIPY **1d** exhibited with 40,000 L mol^{-1} cm^{-1} the smallest extinction coefficient, about one third that of **1a**.

Besides of the star-shaped aza-BODIPY **1d**, all other thienyl-substituted derivatives **1a**–**c** emit in the red spectral region. The corresponding fluorescence spectra were measured quantitatively and are shown in Fig. 1c. As can be seen, the emission maxima vary between 725 nm for **1b** and 764 nm for **1c**. The Stokes shift is in the usual range but it is with 42 nm significantly larger for the compound **1b** than for the other compounds **1a** and **1c** with a Stokes shift of 22 nm only. This data indicate, that the excited state geometries of the compounds **1a** and **1c** have, in contrast to the geometry of compound **1b**, minor differences compared to the corresponding ground state geometries.[19]

2.3. Electrochemical characterization

Both compound series **7a**–**d** and **1a**–**d** as well as compound **8** were analyzed with cyclic voltammetry (CV) to obtain the corresponding oxidation and reduction potentials. The measurements were performed in dichloromethane, using an Ag/AgCl reference electrode with the ferrocene/ferrocinium couple (Fc/Fc^+) as internal redox standard.[20]

All examined compounds exhibit, as shown for the aza-BODIPYs **1a**–**d** in Fig. 2, reversible one-electron reduction and irreversible one-electron oxidation waves. This fact points to the formation of stable radical anions under the applied conditions. The reason for the irreversible oxidation waves might be the unsubstituted 5-position at the thiophene ring, which is known to be reactive and can undergo electrochemical polymerization via the corresponding radical cations.[21]

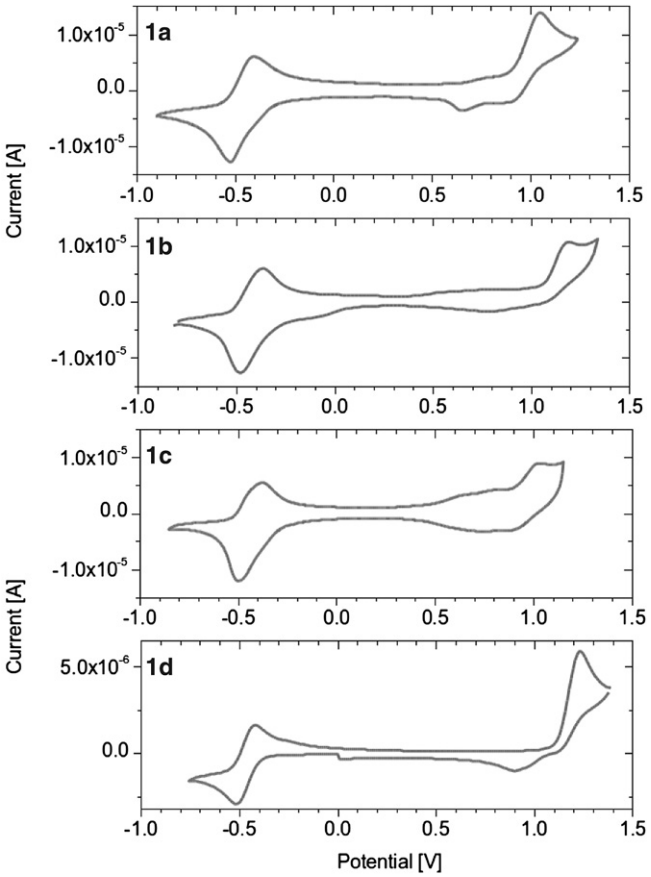

Fig. 2. Cyclic voltammograms of the aza-BODIPYs **1a**–**d** measured in dichloromethane against Ag/Ag^+.

From the redox potentials, listed in Table 2, it can be seen that the boron difluoride-free dipyrroazamethenes **7a**–**d** show the lowest oxidation and reduction potentials.

Table 2
Electrochemical data of the dipyrroazamethines **7a**–**d**, the aza-BODIPYs **1a**–**d**, and **8**

	E_{OX}[a] [V]	E_{RED}[a] [V]	HOMO[b] [eV]	LUMO[b] [eV]	ΔE[c] [eV]
7a	0.41	−1.19	−5.19	−3.59	1.60
7b	0.44	−1.18	−5.22	−3.60	1.62
7c	0.35	−1.16	−5.13	−3.62	1.51
7d	0.65	−1.16	−5.43	−3.62	1.81
8	1.07	−0.72	−5.85	−4.06	1.79
1a	0.68	−0.76	−5.46	−4.02	1.44
1b	0.72	−0.86	−5.50	−3.92	1.58
1c	0.47	−0.84	−5.25	−3.94	1.31
1d	0.90	−0.77	−5.68	−4.01	1.67

[a] Redox-potentials versus Fc/Fc^+ of the first reduction (E_{RED}) and oxidation (E_{OX}); measured in CH_2Cl_2/Bu_4PF_6(0.1 M) versus Ag/AgCl, scan rate 100 mVs^{-1}, with Fc/Fc^+ as internal standard.
[b] Determined HOMO and LUMO energy values.
[c] HOMO–LUMO gap from the obtained redox potentials.[22]

The redox potentials of the aza-BODIPY compounds **1a**–**d** are shifted to higher potentials compared to **7a**–**d**. This effect is caused by the electron withdrawing character of the BF_2 moiety in the aza-BODIPYs **1a**–**d** and leads to a facilitated reduction of these compounds whereas the oxidation becomes less favored. This trend is intensified for the dibromo substituted aza-BODIPY compound **8**, which is easily reducible due to the electron negativity of the bromine substituent.

By using the measured oxidation and reduction potentials, the HOMO and LUMO energies of **7a**–**d** and **1a**–**d** were determined with the potential of Fc/Fc^+ as reference energy and are listed in Table 2. The obtained frontier orbital energies for **1a**–**d** are displayed in Fig. 3. The energetic stabilization caused by the complexation with BF_3 is slightly more pronounced for the LUMO energies than for the HOMO energies, as can be seen by calculating the corresponding **1**(HOMO)–**7**(HOMO) and **1**(LUMO)–**7**(LUMO) differences for **1a**–**d** and **7a**–**d**, respectively. Consequently, the HOMO–LUMO gap ΔE listed in Table 2 for the aza-BODIPYs **1a**–**d** is smaller than for the dipyrroazamethenes **7a**–**d**. This characteristic is in accordance with the trend of the optical absorption measurements (see above).

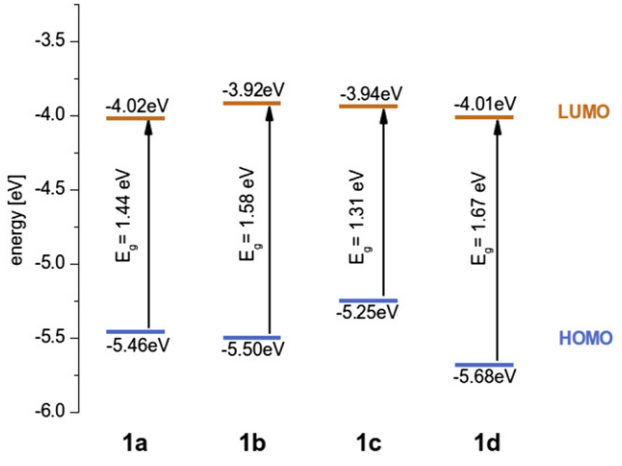

Fig. 3. HOMO and LUMO energy values for the aza-BODIPYs **1a**–**d**, derived from the CV measurements.

Comparing the HOMO energies of the parent aza-BODIPY **2** to the thiophene substituted derivatives **1a**–**d** reveals that the 2,6-dithienyl-substituted compound **1d** has the same HOMO and LUMO energies as **2**, whereas the HOMO energies of the compounds **1a**–**c** are significantly increased. The thiophene substituents at the 3,5-position for **1a** result in an increase of 0.2 eV (in comparison to **2**), whereas at the 1,7-position for **1b** it amounts to 0.16 eV. In **1d** the influence of the thiophene substituents in the 2,6-position on the HOMO energy is negligible, as no differences in the redox potentials can be seen for **1d** compared to **2**.[23] The largest effect was found for the 1,3,5,7-tetrathienyl-substituted aza-BODIPY **1c** with an increased HOMO energy of 0.43 eV compared to **2**. In contrast to the HOMO energies, the LUMO energies of **1a**–**d** stay rather constant with minor changes between 0 and 0.09 eV. This allows a systematically HOMO energy level tuning and, consequently, a control of the band gap by the choice of appropriate substituents in this aza-BODIPY system.

2.4. Quantum chemical calculations

DFT calculations for the aza-BODIPYs **1a**–**d** were performed (at the b3lyp/6-31+g^{**} level of theory)[24] in order to gain a deeper insight into the experimental optical and electrochemical observed structure–property relationship.

The electronic structures of the aza-BODIPYs **1a**–**d** provide some general characteristics for understanding of substituent effects on the electrochemical and optical properties. To discuss this correlation, the HOMO and LUMO orbitals are displayed, exemplarily for **1a** in Fig. 4 (for compound **1b**–**d** see Supplementary data). It can be seen that both the HOMO and LUMO are exclusively characterized as π orbitals, as expected. However, the distributions of the MO coefficients for both frontier orbitals show essential differences.

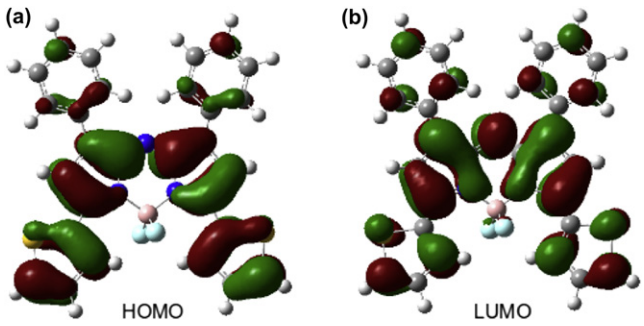

Fig. 4. Froniter orbitals of aza-BODIPY **1a**.

In the LUMO the largest coefficients are localized at the aza-BODIPY core with a strong contribution on the nitrogen atoms and, particularly, at the azamethene bridge (in position 8, shown in Fig. 4b). Corresponding to the larger LUMO coefficient at the nitrogen atoms, the complexation with boron trifluoride has a stronger influence on the LUMO energy. Accordingly, the stabilization of the energy levels due to the electron withdrawing character of the boron difluoride moiety is more pronounced for the LUMO in **1a**. As a consequence, a reduced energetic gap for **1a** compared to **7a** can be recorded by cyclic voltammetry (see above).

In the HOMO orbital (shown in Fig. 4a), the coefficients are small at the pyrrole nitrogen atoms, especially at the azamethene bridge nitrogen atom due to a nodal plane. In contrast, the coefficients at the residual aza-BODIPY core and on the (het)aryl-rings at the 3,5-position are relatively large.

These observations demonstrate that substituents in the 3,5-position at the aza-BODIPY core influence predominantly the HOMO energies in these compounds. Accordingly, the HOMO energies can be increased more effectively than the LUMO energies by attaching electron donating substituents at the aza-BODIPY core.[25] Moreover, this effect is larger at the 3,5-position than at the 1,7-position. Therefore, compound **1a** shows a higher HOMO energy than compound **1b**. In compound **1c**, the overall electron donating

character is enhanced due to the 1,3,5,7-tetrathienyl substitution and the HOMO energy is further increased compared to **1a** and **1b**.

Furthermore, the influence of substituents on the frontier orbital energies depends on the dihedral angle between the aza-BODIPY core and the substituents, as the conjugation decreases with an increasing angle. This was demonstrated by Carreira et al. who synthesized conformational restricted aza-BODIPYs and found a strong bathochromic shift of the absorption maximum compared to the unrestricted compounds.[26] In compound **1d**, the thienyl substituents do not show any influence on the energy levels compared to the 1,3,5,7-tetraphenyl aza-BODIPY **2**. In the case of **1d** a steric hindrance of the thiophenes can be assumed, due to the presence of adjacent phenyl rings at the aza-BODIPY core.

DFT geometry optimizations[24,27] illustrate a propeller-like structure of the peripheral (het)aryl-rings in **1d** with increased dihedral angles between 56° and 60°. In contrast, the thiophene moieties in the compounds **1a**–**c** exhibit smaller dihedral angles between 14° and 19° and the phenyl rings in **1a** and **1b** cause angles between 28° and 36°, respectively. Hence, this result confirms the diminished influence of the thiophene substitution in **1d** due to steric hindrance.[27]

2.5. Calculated frontier orbital energies

The calculated HOMO energies agree well with the energies derived from CV measurements with a maximum difference of only 0.02 eV–0.15 eV, with the largest deviation for **1c** (see Table 2 and Table 3). The differences in the LUMO energies with respect to the experiments are higher, in the order of 0.39–0.54 eV. This originates to some extent from the idealized calculations in gas phase and might be improved slightly by applying an appropriate solvation model.[28]The energies of the absorption maxima of the aza-BODIPYs **1a**–**d** were calculated with the time dependent DFT approach[29] (at the b3lyp/6-31+g** level of theory)[24] and were in good agreement with the experimental value with a tolerance in the range from 0.19 eV to 0.29 eV. These deviations can be attributed to overestimated LUMO energies. However, the predicted oscillator strengths for the absorption maxima reflect the measured trend of the extinction correctly.

The DFT calculations revealed that the UV absorptions of the aza-BODIPYs **1a**–**c** can be ascribed to transitions from the HOMO and some of the lower lying occupied levels (HOMO-1, HOMO-3, HOMO-4) to the LUMO and several higher lying unoccupied levels (LUMO+1, LUMO+2). In accordance with the experiment, no noteworthy oscillator strength in this spectral region was calculated for **1d**. The absorption maxima in the visible range of the compounds **1a**–**c** are predominantly HOMO–LUMO transitions, although other excitations are involved to a minor extent, in case a thiophene unit is present in the 1,7-position as for **1b** and **1c** (see Table 3). Therefore, the experimentally observed bathochromic shifts in the series **1a**–**c** are induced by the reduced HOMO–LUMO gap, as it was already suggested by the CV results.

The star-shaped aza-BODIPY compound **1d** offers a discrepancy compared to **1a**–**c**. Here, two transitions with a HOMO-2→LUMO and HOMO→LUMO component, differing about 0.25 eV in energy, are responsible for the absorption maximum (see Table 3).

Accordingly, the absorption band of **1d** is caused by a superposition of two excitations giving rise to a broadening of the absorption band for the 2,6-dithienyl-substituted aza-BODIPY derivative **1d**.

3. Conclusion

To summarize, a series of novel thiophene-substituted aza-BODIPY dyes has been synthesized via a synthetic standard route extended by a Stille-coupling of a 2,6-dibromo dipyrroazamethene derivative with a stannylated thiophene. The new compounds were systematically characterized in terms of the substitution pattern with both experimental and theoretical methods.

It was found that the absorption maxima of the aza-BODIPY compounds prepared can be shifted into the red spectral region by replacing phenyl with thiophene moieties. This effect can be attributed to an increase of the HOMO energies, while the LUMO energies remain nearly constant, resulting in an overall reduced gap. DFT calculations confirmed the experimental results and displayed predominantly a HOMO–LUMO transition for the absorption, except for the 2,6-thiophene derivative. For this compound, the absorption originates from two overlapping transitions leading to a broad and weak absorbance.

Analysis of the frontier orbitals revealed significant differences in the distribution of the frontier orbital coefficients. According to the distribution of the HOMO coefficients, the influence of the thiophene substituents on the HOMO energies is stronger than on the LUMO energies and varies with the substitution pattern. The largest effect was found for the thiophene substitution at the 1,3,5,7- and 1,5-positions for the bis-thiophene-substituted aza-BODIPY compounds. The thiophene substitution in the 2,6-position has no influence on the optical and electrochemical properties, which originated from weak conjugation caused by steric hindrance.

Particularly with regard to applications, the thiophene-substituted aza-BODIPYs indicate to be suitable for organic solar cells applications because of their intense absorption and tunable energy levels as well as for their reversible reduction. Due to the versatility of the brominated aza-BODIPY compounds in Stille-coupling reaction, as exemplified for compound **8**, numerous other substituted aza-BODIPY derivatives should be easily accessible. New synthetic targets following that direction, together with the testing of the optoelectronic properties, are currently under investigation.

Table 3
Results of the DFT calculations for the aza-BODIPYs **1a**–**d**

	Energy[a] [eV] (nm)	Oscillator strength[a]	Principle orbital contribution[a]	Energy[a] [eV] (nm)	Oscillator strength[a]	Principle orbital contribution[a]	HOMO [eV]	LUMO [eV]	ΔE [eV]
1a	3.73 (331.84)	0.70	HOMO-3→LUMO HOMO→LUMO+1 HOMO→LUMO+2	2.01 (615.11)	0.73	HOMO→LUMO (91%)	−5.44	−3.48	1.96
1b	3.85 (317.26)	0.28	HOMO→LUMO+1 HOMO–LUMO+2	2.01 (614.60)	0.60	HOMO→LUMO (64%) HOMO-1→LUMO (4%)	−5.58	−3.53	2.05
1c	3.59 (344.55)	0.63	HOMO-4→LUMO HOMO→LUMO+1 HOMO→LUMO+2	1.90 (651.57)	0.68	HOMO→LUMO (63%) HOMO-1→LUMO (2%)	−5.39	−3.53	1.86
1d	2.30 (537.83)	0.49	HOMO-2→LUMO (52%) HOMO→LUMO (22%)	2.05 (604.28)	0.32	HOMO-2→LUMO (36%) HOMO→LUMO (48%)	−5.71	−3.47	2.24

[a] The most intense transitions contributing to the absorption spectrum.

4. Experimental and computational details

4.1. General

All necessary starting materials were obtained from commercial sources and used without further purification. Toluene was dried over sodium and distilled right before use or stored over molecular sieve 4 Å. The solvents dichloroethane, dichloromethane, and *n*-butanol were dried over molecular sieves 4 Å. ^{1}H and ^{13}C NMR spectra were recorded in $CDCl_3$ with a Bruker DRX 500 P instrument for 500.13 and 125.76 MHz, respectively. The assignment of quaternary, secondary, and primary C atoms was completed using DEPT spectra. Elemental analyses were estimated with a Eurovektor Hekatech EA-3000 elemental analyzer and the UV–vis spectra with a Perkin Elmer λ 25 spectrometer. The emission spectra were recorded on an Edingburgh spectrometer and the mass spectra with a Bruker Esquire-LC 00084 instrument. Melting points were determined with a Netzsch STA 449C instrument. Cyclic voltammograms were recorded with a Metrohm μ-Autolab instrument in a single-component cell under a nitrogen atmosphere. A typical three electrode configuration with an inlaid platinum disk as working electrode, a platinum wire as counter electrode, and a silver rod coated electrochemically with AgCl was used. The potentials were measured versus Ag/AgCl and referenced to ferrocene as an internal standard ($E^0(Fc/Fc^+)=-4.78$ eV to vacuum). The measurements were performed with a scan rate of 100 mVs^{-1} in degassed dichloromethane (HPLC quality) containing tetra-*n*-butylammonium hexafluorophosphate (TBAPF, 0.1 mol L^{-1}) as electrolyte.

The fluorescence quantum yields Φ were estimated by use the comparative method described by Williams et al.[30] Freshly prepared solutions of Rhodamine 101 as standard in ethanol with five different concentrations and compound **1a**, **1b**, and **1c** in dichloromethane are used for recording the absorption as well as fluorescence spectra using a slit of 5 nm for each sample. The fluorescence quantum yield of Rhodamine 101 is defined to be $\Phi=1$ according to reference.[31,32] The excitation wavelengths for Rhodamine 101 and for the compounds **1a**, **1b**, and **1c** are selected as 550 nm, 655 nm, 630 nm, and 700 nm, respectively. The intensities measured were corrected in each case by the lamp spectra.

With these preconditions the fluorescence quantum yields Φ were calculated by using the following equation in which Grad is defined as the gradient from the plot of the integrated fluorescence intensities over the optical densities at the excitation wavelength and η the reactive index of the solvents:[33]

$$\Phi_X = \Phi_R\left(\frac{Grad_X}{Grad_R}\right)\left(\frac{\eta_X^2}{\eta_R^2}\right)$$

The subscripts X and R refer to the probe and the standard reference solution, respectively.

For all quantum chemical calculations the Gaussian03 package[24] was used and the ab initio calculations of the orbital energies were performed with density functional theory using the b3lyp functional with the basis set 6-31+g(d,p). No symmetry constrains were used for the geometry optimization. All optimized structures were confirmed with subsequent frequency calculations to make sure that a true minimum was reached. The absorption energies and the principal orbital contributions were calculated with time dependent DFT as implemented in the Gaussian package.

4.2. Preparation of the thienyl-substituted chalcones 5 (general procedure)

To a mixture of a (het)arylketone **3** (50 mmol) and a (het) arylaldehyde **4** (50 mmol), dissolved in 25 mL ethanol, potassium hydroxide (0.2 g, 3.56 mmol), dissolved in 5 mL water, was added at rt. The mixture was stirred for 24 h and the products precipitated were filtered of, washed with aqueous ethanol and dried. Recrystallization from ethanol gave **5** as white solids in satisfactory yields. The spectroscopic data for all compounds **5a–d** were in accordance to those reported in the literature.[34]

4.3. Preparation of the dipyrroazamethenes 7a–c (general procedure)

A mixture of a chalcone **5** (100 mmol), nitro methane (500 mmol), and K_2CO_3 (0.2 mmol), dissolved in ethanol (100 mL), was heated to reflux for 6–12 h.[35] After cooling at rt, the solvent was removed in vacuum and the oily residue obtained was dissolved in ethyl acetate and washed with water (3×50 mL). The combined organic layers were washed with brine, dried over sodium sulfate, and concentrated to give the target compounds as a yellowish oily residue in nearly quantitative yields, which were used in the next step without further purification.

A mixture of a 1,3-(bis-(het)aryl)-4-nitrobutanone **6** (1 mmol) and ammonium acetate (20 mmol) was refluxed in *n*-butanol (100 mL) for 24 h. After cooling to rt, the reaction mixture was diluted with water and extracted three times with dichloromethane. The combined organic layers were washed with water and brine, dried with sodium sulfate, and concentrated to give the crude product as a dark blue-black solid. Purification by column chromatography yields the desired products as coppery shiny crystals.

By this procedure, the following compounds were synthesized:

*4.3.1. 3-Phenyl-5-(thienyl-1H-pyrrol-2-yl)-(3-phenyl-5-thienyl-pyrrol-2-ylidene)-amine (**7a**).* In a yield of 8%; mp: 262–263 °C; ^{1}H NMR: ppm=8.03 (d, *J*=7.2 Hz, 4H), 7.60 (d, *J*=3.7 Hz, 2H), 7.50 (d, *J*=4.9 Hz, 2H), 7.41 (t, *J*=7.2 Hz, 4H), 7.34 (t, *J*=7.3 Hz, 2H), 7.19 (t, *J*=3.5 Hz, 2H), 7.06 (s, 2H). ^{13}C NMR: ppm=149.3, 149.0, 142.2, 137.0, 133.5, 129.0, 128.8, 128.7, 128.2, 128.0, 127.3, 114.7. ESI-MS *m*/*z* (%): [M+H] 462.1. Elemental analysis: calcd for $C_{28}H_{19}N_3S_2$: C 72.86, H 4.15, N 9.10, S 13.89; found: C 72.37, H 4.04, N 8.27, S 13.92.

*4.3.2. 5-Phenyl-3-(thienyl-1H-pyrrol-2-yl)-(5-phenyl-3-thienyl-pyrrol-2-ylidene)-amine (**7b**).* In a yield of 6%; mp: 257–260 °C; ^{1}H NMR: ppm=7.91 (d, *J*=7.2 Hz, 4H), 7.86 (d, *J*=2.4 Hz, 2H), 7.52 (t, *J*=7.1 Hz, 4H), 7.46 (d, *J*=7.2 Hz, 3H), 7.42 (d, *J*=4.1 Hz, 2H), 7.15 (t, *J*=4.3 Hz, 2H), 7.09 (s, 2H). ^{13}C NMR: ppm=155.3, 149.1, 136.9, 135.9, 131.9, 130.1, 129.1, 127.9, 127.7, 127.2, 126.5. ESI-MS *m*/*z* (%): [M+H] 462.1. Elemental analysis: calcd for $C_{28}H_{19}N_3S_2$: C 72.86, H 4.15, N 9.10, S 13.89; found: C 72.68, H 3.69, N 9.29, S 13.35.

*4.3.3. 3,5-(Bithienyl-1H-pyrrol-2-yl)-(3,5-bithienyl-pyrrol-2-ylidene)-amine (**7c**).* In a yield of 12%; mp: 312–315 °C; ^{1}H NMR: ppm=7.84 (d, *J*=3.6 Hz, 2H), 7.58 (d, *J*=3.6 Hz, 2H), 7.50 (d, *J*=4.9 Hz, 2H), 7.41 (d, *J*=5.0 Hz, 2H), 7.19 (d, *J*=4.9 Hz, 2H), 7.14 (d, *J*=5.0 Hz, 2H), 6.93 (s, 2H). ^{13}C NMR: ppm=149.2, 148.9, 136.9, 136.6, 135.7, 128.8, 128.7, 127.9, 127.7, 127.4, 127.3, 113.0. ESI-MS *m*/*z* (%): [M+H] 474.0. Elemental analysis: calcd for $C_{24}H_{15}N_3S_4$: C 60.86, H 3.19, N 8.87, S 27.08; found: C 61.23, H 2.77, N 8.21, S 27.10.

4.4. Preparation of the aza-BODIPYs 1a–c (general procedure)

To a solution of a corresponding azamethene derivative **7** (12.6 mmol) in dichloroethane (150 mL) diisopropylamine (10.5 mL, 60.8 mmol) was added and the mixture stirred for

1 h. Then $BF_3 \cdot OEt_2$ (7.5 mL, 60.5 mmol) was added at rt and the resulting mixture refluxed until the starting material was completely converted (ca. 2 h) to the corresponding product (checked with TLC). The cold reaction mixture was diluted with water and extracted twice with dichloromethane (100 mL). The combined organic layers were dried with sodium sulfate and concentrated in vacuum. The crude products were purified by flash chromatography using dichloromethane/hexane as eluent to obtain the products as coppery shiny crystals.

By this procedure, the following compounds were prepared.

4.4.1. Aza-BODIPY ***1a***. In a yield of 78%; mp: 297–298 °C; ^{1}H NMR: ppm=8.37 (d, J=3.8 Hz, 2H), 8.05 (d, J=8.3 Hz, 4H), 7.63 (d, J=4.3 Hz, 2H), 7.42 (m, 3H), 7.27 (t, J=4.0 Hz, 2H), 7.17 (s, 2H). ^{13}C NMR: ppm=149.7, 145.6, 142.8, 134.0, 133.0, 132.1, 131.7, 129.8, 129.3, 129.2, 128.5, 118.6. ESI-MS m/z (%): [M+H] 474.0. Elemental analysis: calcd for $C_{28}H_{18}BF_2N_3S_2$: C 66.02, H 3.56, N 8.25, S 12.59; found: C 66.22, H 3.25, N 7.74, S 11.61.

4.4.2. Aza-BODIPY ***1b***. In a yield of 68%; mp: 272–274 °C; ^{1}H NMR: ppm=7.94 (m, 4H), 7.86 (dd, J=3.6, 0.9 Hz, 2H), 7.51 (dd, J=5.0, 0.9 Hz, 4H), 7.40 (t, J=3.3 Hz, 6H), 7.14 (dd, J=5.0, 1.2 Hz, 2H), 6.84 (s, 2H). ^{13}C NMR: ppm=159.5, 144.9, 138.3, 134.7, 131.5, 130.8, 130.3, 129.7, 129.4, 128.5, 128.3, ESI-MS m/z (%): [M+H] 510.1. Elemental analysis: calcd for $C_{28}H_{18}BF_2N_3S_2$: C 66.02, H 3.56, N 8.25, S 12.59; found: C 66.12, H 3.67, N 7.51, S 12.25.

4.4.3. Aza-BODIPY ***1c***. In a yield of 82%; mp: 318–320 °C; ^{1}H NMR: ppm=7.06 (s, 2H), 7.19 (t, J=5.0 Hz, 2H), 7.25 (t, 2H), 7.55 (d, J=5.0 Hz, 2H), 7.62 (d, J=5.0 Hz, 2H), 7.92 (d, J=3.7 Hz, 2H), 8.34 (d, J=3.8 Hz, 2H). ^{13}C NMR: ppm=151.8, 149.7, 148.2, 134.4, 133.9, 133.0, 131.5, 129.9, 129.7, 129.4, 129.1, 116.2. ESI-MS m/z (%): [M+H] 522.4. Elemental analysis: calcd for $C_{24}H_{14}BF_2N_3S_4$: C 55.28, H 2.71, N 8.06, S 24.60; found: C 54.86, H 2.70, N 7.81, S 25.23.

4.4.4. Synthesis of the aza-BODIPY ***1d***. The dibromo compound **8** (0.2 g, 0.3 mmol), prepared according to Ref. 1, and 2-(tributylstannyl)thiophene (0.24 g, 0.61 g) were dissolved in dry toluene under nitrogen. Tetrakis(triphenylphosphine)palladium(0) (0.14 g, 0.1 mmol) was added and the mixture refluxed over night, until no starting material could be detected by TLC. The reaction mixture was cooled to rt and evaporated to dryness. Purification by column chromatography with chloroform yielded the product **1d** in a yield of 85% (169 mg); mp: >320 °C; ^{1}H NMR: ppm=6.62 (dd, J=3.6, 1.1 Hz, 2H), 6.85 (dd, J=5.1, 3.6 Hz, 2H), 7.20 (dd, J=5.1, 1.1 Hz, 2H), 7.31 (m, 8H), 7.34 (t, J=7.4 Hz, 4H), 7.53 (d, J=7.2 Hz, 4H), 7.54 (d, J=6.8 Hz, 4H). ^{13}C NMR: ppm=159.6, 145.1, 142.0, 133.5, 131.2, 130.9, 130.1, 130.0, 128.8, 128.7, 127.8, 127.7, 127.0, 126.8, 126.4, 125.8. ESI-MS m/z (%): [M+H] 662.3. Elemental analysis: calcd for $C_{40}H_{26}BF_2N_3S_2$: C 72.62, H 3.96, N 6.35, S 9.69; found: C 72.86, H 3.70, N 6.13, S 9.23.

Acknowledgements

The authors gratefully acknowledge the financial support by the German Bundesministerium für Bildung und Forschung (BMBF) within the Innoprofile program (03IP602) and the computational resources provided by the Center for Information Services and High Performance Computing (ZIH), TU Dresden.

Supplementary data

Supplementary data associated with this article can be found in the online version, at doi:10.1016/j.tet.2011.06.100.

References and notes

1. (a) Ziessel, R.; Ullrich, G.; Harriman, A. *New J. Chem.* **2007**, *31*, 496–501; (b) Loudet, A.; Burgess, K. *Chem. Rev.* **2007**, *107*, 4891–4932; (c) Wood, T. E.; Thompson, A. *Chem. Rev.* **2007**, *107*, 1831–1861.
2. (a) Urano, Y.; Asanuma, D.; Hama, Y.; Koyama, Y.; Barrett, T.; Kamiya, M.; Nagano, T.; Watanabe, T.; Hasegawa, A.; Choyke, P. L.; Kobayashi, H. *Nat. Med.* **2009**, *15*, 104–109; (b) Lee, J.-S.; Kang, N.-Y.; Kim, Y. K.; Samanta, A.; Feng, S.; Kim, H. K.; Vendrell, M.; Park, J. H.; Chang, Y.-T. *J. Am. Chem. Soc.* **2009**, *131*, 10077–10082.
3. Hepp, A.; Ulrich, G.; Schmechel, R.; von Seggern, H.; Ziessel, R. *Synth. Met.* **2004**, *146*, 11–15.
4. (a) Rousseau, T.; Cravino, A.; Bura, T.; Ulrich, G.; Ziessel, R.; Roncali, J. *Chem. Commun.* **2009**, 1673–1675; (b) Rousseau, T.; Cravino, A.; Bura, T.; Ulrich, G.; Ziessel, R.; Roncali, J. *J. Mater. Chem.* **2009**, *19*, 2298–2300.
5. (a) Rogers, M. A. T. *J. Chem. Soc.* **1943**, 590–596; (b) Davies, W. H.; Rogers, M. A. T. *J. Chem. Soc.* **1944**, 126–131; (c) Knott, E. B. *J. Chem. Soc.* **1947**, 1196–1201.
6. Hall, M. J.; McDonnell, S. O.; Killoran, J.; O'Shea, D. F. *J. Org. Chem.* **2005**, *70*, 5571–5578.
7. (a) Killoran, J.; Allen, L.; Gallagher, J.; Gallagher, W. M.; O'Shea, D. F. *Chem. Commun.* **2002**, 1862–1863; (b) McDonnell, S. O.; Hall, M. J.; Allen, L. T.; Byrne, A.; Gallaher, W. M.; O'Shea, D. F. *J. Am. Chem. Soc.* **2005**, *127*, 16360–16361; (c) Quartarolo, A. D.; Russo, N.; Sicilia, E. *Chem.—Eur. J.* **2006**, *12*, 6797–6803; (d) Adarsh, N.; Avirah, R. R.; Ramaiah, D. *Org. Lett.* **2010**, *12*, 5720–5723.
8. (a) Zhao, W.; Carriera, E. M. *Angew. Chem., Int. Ed.* **2005**, *44*, 1677–1678; (b) Loudet, A.; Bandichhor, R.; Wu, L.; Burgess, K. *Tetrahedron* **2008**, *64*, 3642–3654; (c) Loudet, A.; Bandichhor, R.; Burgess, K.; Palma, A.; McDonnell, S. O.; Hall, M. J.; O'Shea, D. F. *Org. Lett.* **2008**, *10*, 4771–4774; (d) Li, Y.; Dolphin, D.; Patrick, B. O. *Tetrahedron Lett.* **2010**, *51*, 811–814.
9. Coskun, A.; Yilmaz, D.; Akkaya, E. U. *Org. Lett.* **2007**, *9*, 607–609.
10. (a) Palma, A.; Tasor, M.; Frimannsson, D. O.; Vu, T. T.; Méallet-Renault, R.; O'Shea, D. F. *Org. Lett.* **2009**, *11*, 3638–3641; (b) Yoshii, R.; Nagai, A.; Chujo, Y. *J. Polym. Sci., Part A: Polym. Chem.* **2010**, *48*, 5348–5356.
11. (a) Schmidt, E. Y.; Trovimov, B. A.; Mikhaleva, A. I.; Zorina, N. V.; Protzuk, N. I.; Petrushenko, K. B.; Ushakov, I. A.; Dvorko, M. Y.; Méallet-Renault, R.; Clavier, G.; Vu, T. T.; Tran, H. T. T.; Pans, R. B. *Chem.—Eur. J.* **2009**, *15*, 5823–5830; (b) Zrig, S.; Rémy, P.; Andrioletti, B.; Rose, E.; Asselberghs, I.; Clays, K. *J. Org. Chem.* **2008**, *73*, 1563–1566; (c) Collado, D.; Casado, J.; Rodríguez González, S.; López Navarrete, J. T.; Suau, R.; Perez-Inestrosa, E.; Pappenfus, T. M.; Raposo, M. M. M. *Chem.—Eur. J.* **2011**, *17*, 498–507; (d) Rihn, S.; Retailleau, P.; Bugsaliewicz, N.; DeNicola, A.; Ziessel, R. *Tetrahedron Lett.* **2009**, *50*, 7008–7013; (e) Gresser, R.; Hummert, M.; Hartmann, H.; Leo, K.; Riede, M. *Chem.—Eur. J.* **2011**, *17*, 2939–2947.
12. (a) Ulrich, G.; Goeb, S.; De Nicola, A.; Retailleau, P.; Ziessel, R. *Synlett* **2007**, 1517–1520; (b) Benniston, A. C.; Copley, G.; Harriman, A.; Rewinska, D. B.; Harrington, R. W.; Clegg, W. *J. Am. Chem. Soc.* **2008**, *130*, 7174–7175; (c) Goeb, S.; Ziessel, R. *Tetrahedron Lett.* **2008**, *49*, 2569–2574.
13. Forgie, J. C.; Skabara, P. J.; Stibor, I.; Vilela, F.; Vobecka, Z. *Chem. Mater.* **2009**, *21*, 1784–1786.
14. (a) Choi, S. H.; Pang, K.; Kim, K.; Churchill, D. G. *Inorg. Chem.* **2007**, *46*, 10564–10577; (b) Choi, S. H.; Kim, K.; Jeo, J.; Meka, B.; Bucella, D.; Pang, K.; Khatu, S.; Lee, J.; Churchill, D. G. *Inorg. Chem.* **2008**, *47*, 11071–11083; (c) Kim, K.; Jo, C.; Easwaramoorti, S.; Sung, J.; Kim, D. H.; Churchill, D. G. *Inorg. Chem.* **2010**, *49*, 4881–4894.
15. Goeb, S.; Ziessel, R. *Org. Lett.* **2007**, *9*, 737–740.
16. *Organikum*, 23 ed.; Schwetlick, K., Ed.; Wiley-VCH: Weinheim, 2009.
17. Gorman, A.; Killoran, J.; O'Shea, C.; Kenna, T.; Gallagher, W. M.; O'Shea, D. F. *J. Am. Chem. Soc.* **2004**, *126*, 10619–10631.
18. Treibs, A.; Kreuzer, F. H. *Liebigs Ann. Chem.* **1968**, *718*, 208–223.
19. Klessinger, M.; Michl, J. *Excited States and Photochemistry of Organic Molecules*; J. Wiley: New York, NY, 1995.
20. Heinze, J. *Angew. Chem.* **1984**, *96*, 823–840.
21. Roncali, J. *Chem. Rev.* **1992**, *92*, 711–738.
22. By using the oxidation and reduction potentials of the compounds, the HOMO and LUMO energies have been calculated with the potential of Fc/Fc^+ as reference energy taken from Connelly, N. G.; Geiger, W. E. *Chem. Rev.* **1996**, *96*, 877–910 as $E_{HOMO}(Fc)=-4.78$ eV: $E_{HOMO}=-4.78-E_{OX}$; $E_{LUMO}=-4.78-E_{RED}$.
23. A detailed comparison of **1d**, **2** and **8**, including the absorption spectra and the cyclic voltammograms is shown in the Supplementary data.
24. Frisch, M. J.; Trucks, G. W.; Schlegel, H. B.; Scuseria, G. E.; Robb, M. A.; Cheeseman, J. R.; Montgomery, J. A.; Vreven, T., Jr.; Kudin, K. N.; Burant, J. C.; Millam, J. M.; Iyengar, S. S.; Tomasi, J.; Barone, V.; Mennucci, B.; Cossi, M.; Scalmani, G.; Rega, N.; Petersson, G. A.; Nakatsuji, H.; Hada, M.; Ehara, M.; Toyota, K.; Fukuda, R.; Hasegawa, J.; Ishida, M.; Nakajima, T.; Honda, Y.; Kitao, O.; Nakai, H.; Klene, M.; Li, X.; Knox, J. E.; Hratchian, H. P.; Cross, J. B.; Bakken, V.; Adamo, C.; Jaramillo, J.; Gomperts, R.; Stratmann, R. E.; Yazyev, O.; Austin, A. J.; Cammi, R.; Pomelli, C.; Ochterski, J. W.; Ayala, P. Y.; Morokuma, K.; Voth, G. A.; Salvador, P.; Dannenberg, J. J.; Zakrzewski, V. G.; Dapprich, S.; Daniels, A. D.; Strain, M. C.; Farkas, O.; Malick, D. K.; Rabuck, A. D.; Raghavachari, K.; Foresman, J. B.; Ortiz, J. V.; Cui, Q.; Baboul, A. G.; Clifford, S.; Cioslowski, J.; Stefanov, B. B.; Liu, G.; Liashenko, A.; Piskorz, P.; Komaromi, I.; Martin, R. L.; Fox, D. J.; Keith, T.; Al-Laham, M. A.; Peng, C. Y.; Nanayakkara, A.; Challacombe, M.; Gill, P. M. W.; Johnson, B.; Chen, W.; Wong, M. W.; Gonzalez, C.; Pople, J. A. *Gaussian 03, Revision E.01*; Gaussian,: Wallingford CT, 2004.
25. Fabian, J.; Hartmann, H. *Light Absorption of Organic Colorants*; Springer: Berlin, Heidelberg, 1980.

26. Zhao, W.; Carreira, E. M. *Chem.—Eur. J.* **2006**, *12*, 7254–7263.
27. See the Supporting Data for cartesian coordinates of the optimized molecular geometries of the aza-BODIPYs **1a**–**d**.
28. (a) Szabo, A.; Ostlund, N. S. *Modern Quantum Chemistry*; Doverl: Mineola, New York, NY, 1996; (b) Cramer, C. J. *Essentials of Computational Chemistry: Theories and Models*, 2nd ed.; Wiley-VCH: Weinheim, 2004.
29. The TD-DFT approach has proven to be superior compared to semi-empirical methods; see Fabian, J. *Dyes Pigm.* **2010**, *84*, 36–53.
30. Williams, A. T. R.; Winfield, S. A.; Miller, J. N. *Analyst* **1983**, *108*, 1067–1071.
31. Karstens, T.; Kobs, K. *J. Phys. Chem.* **1980**, *84*, 1871–1872.
32. Rurack, K.; Spieles, M. *Anal. Chem.* **2001**, *83*, 1232–1242.
33. Lakowicz, J. R. *Principles of Fluorescence Spectroscopy*, 2nd ed.; Kluwer Academic/Plenum: New York, NY, London, Moscow, Dordrecht, 1999.
34. (a) Koa, H.-H.; Tsaob, L.-T.; Yuc, K.-L.; Liuc, C.-T.; Wangb, J.-P.; Lin, C.-N. *Bioorg. Med. Chem.* **2003**, *11*, 105–111; (b) Ramesh, B.; Someswara Rao, B. *E-J. Chem.* **2010**, *7*, 433–436; (c) Dannhardta, G.; Kiefera, W.; Krämera, G.; Maehrleina, S.; Nowea, U.; Fiebich, B. *Eur. J. Med. Chem.* **2000**, *35*, 499–510.
35. Peseke, K.; Götze, L.; Reinke, H.; Cedeño, Q. A.; Quincoces Suarez, J.; Gomez Andreu, M.; Vélez Castro, H. *J. Prakt. Chem.* **1997**, *339*, 656–659.